

Adhesion Force Detection Method Based on the Kalman Filter for Slip Control Purpose

DOI 10.7305/automatika.2016.10.1152
UDK 681.532.6.015.44-026.569:629.42.015.067.4-047.58

Original scientific paper

The slip control is important for an adhesion force transmission between locomotive wheels and rails. The slip control consists of two tasks. The first task is the slip value detection and the second one is the evaluation of a slip value with a subsequent control action. These two tasks can be realized by many types of methods. Several detection methods use an adhesion coefficient or the adhesion force determination. Because of difficulty of the adhesion coefficient measurement during the train run the adhesion coefficient or the adhesion force has to be estimated. In this paper, the adhesion force is estimated by the Kalman filter. The Kalman filter uses the locomotive model and measured locomotive velocity. The Kalman filter is implemented in Matlab and also applied on measured data.

Key words: adhesion, Kalman filter, locomotive mathematical model, slip control

Detekcija adhezijske sile korištenjem Kalmanovog filtra u svrhe upravljanja proklizavanjem. Upravljanje proklizavanjem bitno je zbog prijenosa adhezijske sile između kotača i tračnica na lokomotivi. Upravljanje proklizavanjem sastoji se od dva zadatka. Prvi je određivanje iznosa proklizavanja a drugi se sastoji od evaluacija iznosa proklizavanja kroz upravljačke akcije. Navedeni zadaci mogu biti ostvareni koristeći više metoda. Nekoliko metoda se koristi za određivanje adhezijskih koeficijenata ili za određivanje adhezijske sile. Zbog poteškoća prilikom mjerenja adhezijskih koeficijenata ili adhezijske sile tijekom rada vlaka, te veličine je potrebno estimirati. U ovome radu adhezijska sila estimirana je korištenjem kalmanovog filtra koji koristi model lokomotive i mjerenja brzine lokomotive. Filtar je implementiran u Matlabu te je korišten na izmjerenim podacima.

Ključne riječi: adhezija, kalmanov filter, matematički model lokomotive, upravljanje proklizavanjem

1 INTRODUCTION

Railway traction vehicles can have problems with the force transmission between wheels and rails. The problems typically occur when the adhesion coefficient decreases due to adverse conditions on the rail surface. Other problems can occur if the vehicle has to transfer high force between wheels and rails during vehicle pulling away or during going uphill. The problems more frequently occur in case of a freight train hauled by a locomotive. Therefore, almost every modern locomotive has a slip controller that provides the maximum force transmission if it is needed.

There are many types of slip control methods described in papers. For slip control, the first order observer [1], [2] or high order disturbance observer [3] could be used. The observers are intended to estimate the adhesion coefficient value. The method which is described in [4] estimates an adhesion force to avoid the problem with an axle weight change during a railway vehicle motion. Work [5] takes into account an axle weight change to reduce the induced wheel slip. A hybrid slip control method is described in

[6]. This method is based on a pattern control method and a speed difference control method. A different approach is described in [7]. This method is based on the different wheelset dynamic behaviour when the different conditions occur in the wheel-rail contact.

The slip controller must solve two tasks. The first task is to detect the beginning of a slip velocity increasing and the second one is to do some control action to limit or stop the slip velocity increasing. In this paper, the adhesion force detection method is proposed and presented. This method does not control the slip velocity by a changing of a motor torque because the slip control is another task. The proposed detection method uses the Kalman filter to predict the adhesion force between wheels and rails on driven wheelset. The control action could be done, e.g. according to a changing of the adhesion force on the slip velocity. The filter input is the wheelset velocity only. The motor torque, as well as the adhesion force, is assumed as a noise. This method is applied to measured data at the locomotive.

2 FORCE TRANSMISSION

The value of the adhesion force that is transmitted between wheels and rails depends on the adhesion coefficient value and adhesion weight. The relation between these parameters is shown in Fig. 1 and the relation is described in (1).

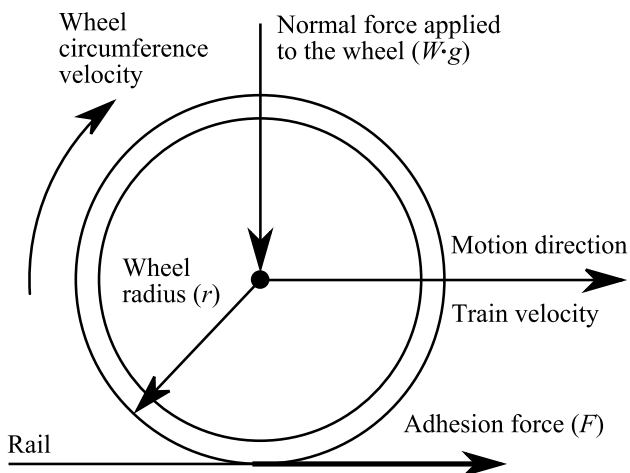


Fig. 1. Forces and velocities that are applied on driven wheel

$$F = \mu \cdot W \cdot g \tag{1}$$

In (1) F is the adhesion force, μ is the adhesion coefficient, W is the adhesion weight and g is gravity acceleration.

The adhesion coefficient value depends on many parameters, e.g. the slip velocity, conditions of the rail surface, train velocity or temperature in the contact area between wheel and rail. The slip velocity is the difference between the wheel circumference velocity and the wheel longitudinal velocity. The adhesion coefficient is a value that could be controlled by a locomotive controller and therefore the adhesion force is controlled by control of the slip velocity. The typical dependence of the adhesion coefficient on the slip velocity is shown in Fig. 2.

3 LOCOMOTIVE MODEL

The Kalman filter needs a system model to correct its work. There are different models described in literature. The described models are of different complexity. On one hand, a couple of models are very complex because they try to describe a large number of locomotive dynamic behaviours. On the other hand, there are very simple models that capture the most significant locomotive behaviour only

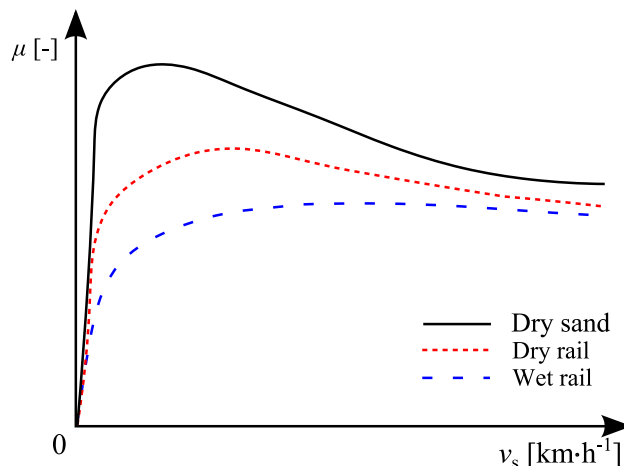


Fig. 2. Example of adhesion coefficient – slip velocity characteristic

[8], [9]. More complex models typically describe the entire locomotive and they need many types of information about the locomotive. Simpler models typically describe only the torque transfer from a motor to a wheelset and the adhesion force transfer between wheels and rails. The simplest model describes locomotive as a torque source and one wheel [10]. The common feature of the models is torque transmission to the wheel with respecting damping and stiffness of elements that are between motor and wheels. The models typically contain three or two masses only.

The models are different because of different simulation purpose. If the model is intended for the verification of slip controller properties or performance it contains an adhesion characteristic calculation [10]. When the models are intended for e.g. the Kalman filter or observer design they do not contain the adhesion characteristic.

The proposed model aims to detect the adhesion force between wheels and rails by using of Kalman filter. Further, the model is intended to be implemented in micro-controller in the future. Therefore, the used model can be simple without any adhesion characteristic calculation. The proposed model has three masses and it describes the torque transmission from the motor to wheels through elastic elements.

3.1 Locomotive description

The measurement has been done on an electric locomotive. Mentioned locomotive is intended to haul freight train with overall weight up to 1500 tonnes. A big value of the slip velocity occurs regularly when the locomotive hauls the train up to a steep hill, especially during the bad condition of a rail surface. The discussed locomotive has

Table 1. Locomotive specification

Parameter	Value
Locomotive mass	123 t
Nominal power	5220 kW
Nominal / maximal speed	50 km·h ⁻¹ / 95 km·h ⁻¹
Tractive effort at 50 km·h ⁻¹	355 kN
Number of wheelsets / bogies	6 / 3

three bogies, and every bogie has two wheelsets. Some locomotive specifications are in Table 1.

Every wheelset is driven by a DC motor. Two motors in one bogie are connected in series, and they are supplied from one inverter. The conception disadvantage is to get the motor torque because the motor torque is available for the entire bogie and the torque for each motor cannot be recognized. Therefore, the slip control methods that need the torque value for the proper work cannot be applied. On every driven wheelset, an incremental encoder for the speed measurement is mounted. The encoders are mounted on one locomotive side but the wheelsets are in the reverse position in the bogie. Therefore, the incremental encoder is mounted in one wheelset on a directly driven wheel and in the second one it is mounted on an indirectly driven wheel side. The situation is shown in Fig. 3. Between the motor shaft and wheelset a gear box with the gear ratio 81:18 is mounted.

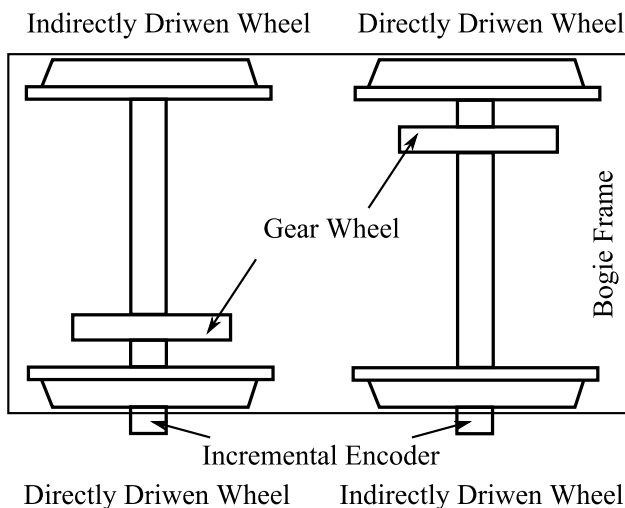


Fig. 3. Bogie schema

Electrical, mechanical and drive locomotive diagram is shown in Fig. 4. In the figure, the bogie mechanical and electrical part and the locomotive control unit are shown. In the electrical part, a power converter, DC motors, gearboxes and incremental encoders are shown. The encoder is mounted on the wheelset that is not shown in the figure.

The control unit contains several interconnected computers. The unit calculates the torque for both motors and it provides the measuring and filtering of the wheelset speed. Both values are sent via control computer to a monitor unit.

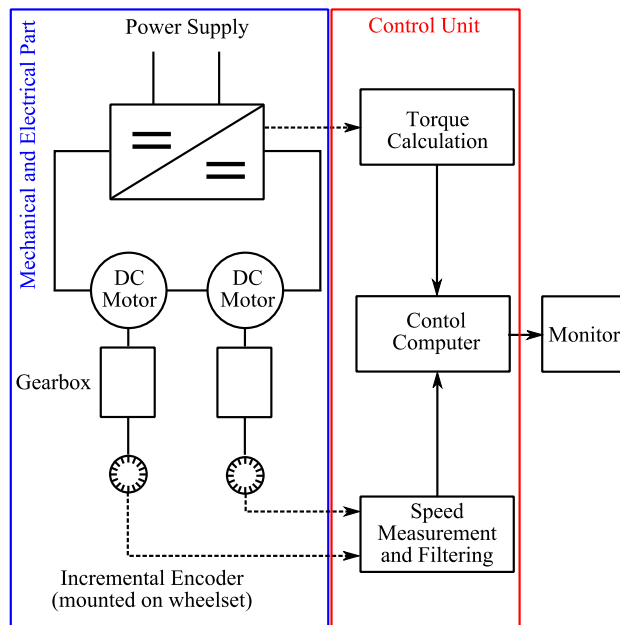


Fig. 4. Locomotive electric diagram

3.2 Locomotive Model

The Kalman filter requires one wheelset model only. The model considers the torque transmission from the motor through the transmission to the directly driven wheel that is nearer to gear wheel and to the indirectly driven one that is further to gear wheel. The wheelset configuration that is used for the wheelset model is shown in Fig. 5. In Fig. 6, the torque transmission from the motor to the contact area between wheels and rails is shown. The torque is transmitted through the elastic elements that have the damping d and stiffness c . Every element has the different value of the damping and stiffness. The motor is connected to the wheelset through the gearbox. The main difference between directly driven wheel and indirectly driven one is in elements that connect wheels with the gear wheel. Both elements have different damping and stiffness. Actions that occur in the gearbox are neglected.

The configuration in Fig. 5 has five masses. The configuration mechanical equation is based on [11], but the equations have to be modified because the model in [11] is intended for the slip controller performance verification and therefore the model consists of additional components that are not needed for the Kalman filter. The problem of

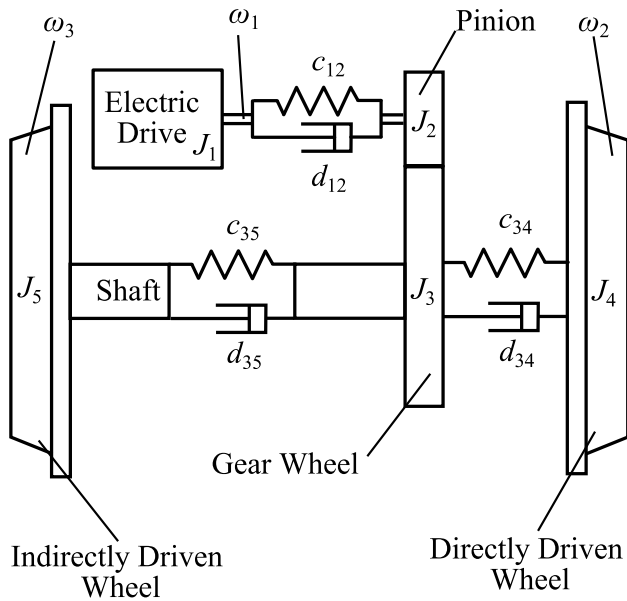


Fig. 5. Wheelset configuration with electric drive

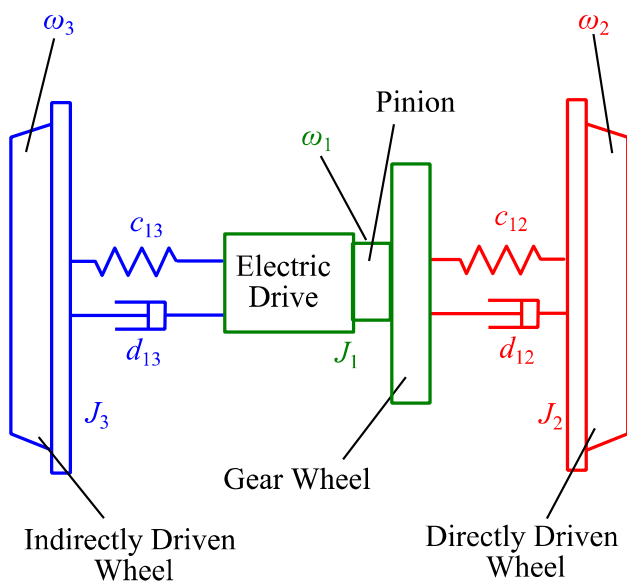


Fig. 6. Reduced model with connected mass

the five mass model is that the model is not fully observable. Therefore, the model contains spare information that is not needed, and the model is unnecessary complicated. Some part of the model has to be reduced to get a simpler model. The reduced model configuration is in Fig. 6.

The reduced model contains three masses. The pinion with a DC motor creates one mass. The second mass creates directly driven wheel connected with a gear wheel, and third mass create indirectly driven wheel. Between masses

are elastic elements with damping d and stiffness c . The coefficients for elements placed between the motor and directly driven wheel and indirectly driven one are different. The three mass model was chosen because the incremental encoder could be on both sides of the wheelset. Both wheels have slightly different behaviour.

The locomotive three mass model state equations for continuous time are:

$$\frac{d}{dt} \begin{bmatrix} \omega_1 \\ \omega_2 \\ \omega_3 \\ T_{12} \\ T_{13} \\ T_A \end{bmatrix} = A \cdot \begin{bmatrix} \omega_1 \\ \omega_2 \\ \omega_3 \\ T_{12} \\ T_{13} \\ T_A \end{bmatrix} \quad (2)$$

where A is

$$\begin{bmatrix} 0 & 0 & 0 & \frac{1}{J_1} & \frac{1}{J_1} & 0 \\ 0 & 0 & 0 & \frac{1}{J_2} & 0 & -\frac{1}{J_2} \\ 0 & 0 & 0 & 0 & \frac{1}{J_3} & -\frac{1}{J_3} \\ c_{12} & -c_{12} & 0 & -\frac{d_{123}}{J_2} & \frac{d_{12}}{J_2} & -\frac{d_{12}}{J_2} \\ c_{13} & 0 & -c_{13} & \frac{d_{13}}{J_3} & -\frac{d_{123}}{J_3} & -\frac{d_{13}}{J_3} \\ 0 & 0 & 0 & 0 & 0 & -\frac{1}{T} \end{bmatrix}$$

In (2) ω_1 is the rotor angular velocity recalculated to wheelset, ω_2 and ω_3 are the directly driven wheel angular velocity and indirectly driven wheel angular velocity. T_{12} and T_{13} are torques between the motor and the directly driven wheel and the indirectly driven one respectively, T_A is the estimated adhesion torque, J_1 , J_2 and J_3 are the moments of inertia, c_{12} and c_{13} are stiffness, d_{12} and d_{13} are the damping between motor and directly driven wheel and indirectly driven one respectively, $d_{123} = d_{12} + d_{13}$ and T is the electric drive constant.

The system output is calculated according to:

$$y = [0 \ 1 \ 0 \ 0 \ 0 \ 0] \quad (3)$$

The state vector in (2) contains the motor and wheels angular velocities ω_1 , ω_2 and ω_3 , torques between motor and wheels T_{12} and T_{13} , and adhesion torque T_A that could be recalculated to the adhesion force. The torques T_{12} and T_{13} are used instead of three swivelling angles φ . The torques are used because the model is unobservable. Therefore, the angles are recalculated to its difference $\varphi_1 - \varphi_2$ and $\varphi_1 - \varphi_3$. The reduced model is fully observable now. Finally, the difference is recalculated to torques T_{12} and T_{13} . The adhesion torque T_A is added to the model to make the calculation of the adhesion torque possible. The adhesion torque is not a part of the locomotive mechanical model.

The five mass model is more precise than the three mass model. The reduction of the model changes its behaviour and it's precise as well. Before the reduction process is done it is needed to decide which system behaviour should be maintained. The used reduction takes into account the system eigenfrequencies. There was detected two eigenfrequencies of 18 Hz and 61 Hz in measured data. Therefore, the reduced model is designed to respect these eigenfrequencies. Bode plot that shows comparison between five mass model and three mass model is shown in Fig. 7.

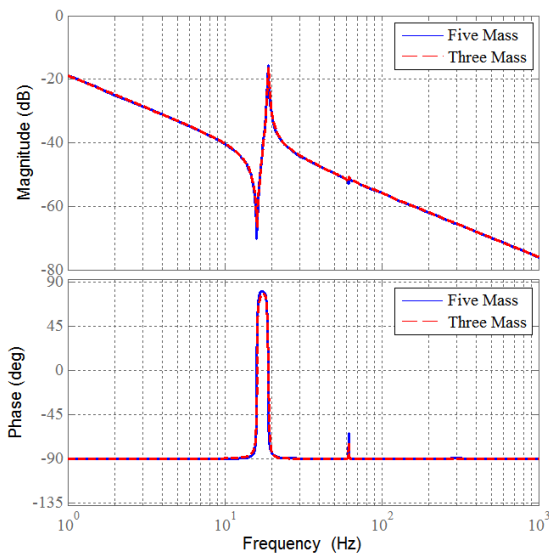


Fig. 7. Bode characteristics of five mass model and three mass model

In Fig 7, it is shown that the magnitude and phase in Bode characteristics are identical to approximately 300 Hz. The frequency 307 Hz is the third eigenfrequency of five mass model according to the Bode characteristic. This eigenfrequency is not taken into account in three mass model. The bode characteristics are identical for both models. The models have the identical behaviour in the time simulation.

4 DETECTION METHOD

The detection method is intended for the estimation of the adhesion force that is transmitted between wheels and rails by one wheelset. For the estimation, the Kalman filter with the locomotive model is used. The model is based on equation (2) that is modified to form with swivelling angles.

4.1 Kalman filter

The general equations for a continuous time dynamic system model are:

$$\frac{d}{dt}x(t) = A \cdot x(t) + B \cdot u(t) + w(t) \quad (4)$$

$$y(t) = C \cdot x(t) + v(t) \quad (5)$$

where x is the state vector, u are known control inputs, w are random dynamic disturbances, y are sensor outputs, v is random sensor noise, A is system matrix, B is input matrix and C is output matrix.

The system contains neither matrix B nor input because the motor torque that is applied by the motor is not available. Then, the used Kalman filter algorithm [12] does not use input u . In the algorithm, the inputs are considered as a part of the dynamic disturbance w . The Kalman filter algorithm is:

$$K_k = \frac{P_k(-) \cdot H_k^T}{H_k \cdot P_k(-) \cdot H_k^T + R} \quad (6)$$

$$\hat{x}_k(+) = \hat{x}_k(-) + K_k \cdot (z_k - H_k \cdot \hat{x}_k(-)) \quad (7)$$

$$P_k(+) = (I - K_k \cdot H_k) \cdot P_k(-) \quad (8)$$

$$\hat{x}_k(-) = \phi_{k-1} \cdot \hat{x}_{k-1}(+) \quad (9)$$

$$P_k(-) = \phi_{k-1} \cdot P_{k-1}(+) \cdot \phi_{k-1}^T + Q_{k-1} \quad (10)$$

$$P_k(-) = \frac{1}{2}(P_k(-) + P_k^T(-)) \quad (11)$$

where K is the Kalman gain matrix, P is state estimation uncertainty covariance matrix, H is measurement sensitivity matrix, R is measurement uncertainty covariance matrix, x_h is system state vector, z_n are measured values, ϕ is system matrix in discrete time and Q is process noise covariance matrix. Subscripts $k(+)$ means a-posteriori estimate, $k(-)$ means a-priori estimate.

The eq. (6) minimizes the mean estimation square error of the state vector to lead the process to its optional state by minimizes error of the state estimation uncertainty covariance matrix. The value of the Kalman gain matrix depends on the measurement uncertainty matrix R . It depends on the measurement signal.

The locomotive model matrix A , according to (2), is in continuous time. For the proper work, the model has to run in continuous time. The equations in continuous time could be used for the Kalman – Bucy filter. However, for the Kalman filter in discrete time, the equations have to be transformed to the discrete time form. The system matrix A , a covariance matrix of process noise Q and a covariance matrix of measurement uncertainty R have to be recalculated to the discrete time model. The transformation could be done as:

$$\phi_{k-1} = \exp\left(\int_{t_{k-1}}^{t_k} A(s)ds\right) \quad (12)$$

$$Q_{k-1} = \phi_{(t_k, t_{k-1})} \left(\int_{t_{k-1}}^{t_k} \phi_{(t_k, t_{k-1})}^{-1} \cdot Q(s) \cdot \phi_{(t_k, t_{k-1})}^{-1} ds \right) \phi_{(t_k, t_{k-1})}^T \quad (13)$$

$$R_k = \frac{1}{t_k - t_{k-1}} \int_{t_{k-1}}^{t_k} R(t)dt \quad (14)$$

4.2 Covariance matrices set

For the Kalman filter proper work, it is needed to set the covariance matrix of measurement noise R and covariance matrix of process noise Q . The Kalman filter performance depends on the matrices settings. If the matrices are set incorrectly the inappropriate results could be obtained. The matrix R size is $(l \times l)$ where C matrix size is $(l \times n)$. The size of the matrix Q is the same as the size of the matrix ϕ . Both matrices are diagonal. Due to various sources of errors, it is difficult to solve the matrix elements analytically. The matrices are set according the simulation results and required output values. The used continuous time process noise matrix Q has form:

$$Q_t = \begin{bmatrix} q_1 & 0 & 0 & 0 & 0 & 0 \\ 0 & q_2 & 0 & 0 & 0 & 0 \\ 0 & 0 & q_3 & 0 & 0 & 0 \\ 0 & 0 & 0 & q_4 & 0 & 0 \\ 0 & 0 & 0 & 0 & q_5 & 0 \\ 0 & 0 & 0 & 0 & 0 & q_6 \end{bmatrix}$$

In the process, noise covariance matrix coefficients are q_1 to q_6 . Every coefficient influences different filter property. The coefficient q_1 influences the filtration of the input signal z_n . The coefficient setting is related to the R matrix value. If the matrix R is increased then the input signal filtration increases and vice versa. If the q_1 is increased then the input signal filtration decreases and vice versa. This behaviour is because of the speed ω_1 is connected to the system input. The coefficient q_2 causes the filter output signal waveform changes. The influence of the coefficient

is caused by speed measurement connection to the speed ω_2 . If the speed measurement is connected to ω_3 then the coefficient q_3 causes signal waveform change. But, the matrices Q and R have to be changed in this case. Other coefficients q_3 to q_6 have slight influence on the output signal.

5 MEASURED DATA AND KALMAN FILTER TUNING

The data were measured on a freight locomotive. During the locomotive motion, some slips occur. The rail was dry during the measurement. The measurement with the slip was done on a railway with a rising gradient. During measurement, every wheelset velocity and first and third bogie tractive effort were measured. The second bogie power supply was switched off. Therefore, the second bogie velocity could be considered as the train velocity reference.

An example of the velocity measured data and calculated tractive effort are shown in Fig. 8. The measured period is 25 seconds long, and it contains one high value of the slip velocity. A driven wheelset velocity and tractive effort of the corresponding bogie is shown. The tractive effort is calculated by the locomotive computer and the tractive effort for one wheelset has approximately half value than value that is shown in the figure. Further, one high value of the slip velocity is worth noticing. The action of the readhesion controller is apparent from the waveform of the tractive effort. The locomotive was equipped with the readhesion controller to avoid high value of the slip velocity because higher wear of wheels and rails occurs during high slip and it can cause the damage of some locomotive parts. The applied tractive effort is constant at the beginning. The locomotive velocity increases when approximately at time 7 s the velocity abruptly increases. Then, the locomotive readhesion controller reacts and decreases the tractive effort to limit the velocity. Then, the tractive effort is increased up to the previous value. The readhesion controller action causes incorrect behaviour of the Kalman filter because of quick fall of the tractive effort which the filter is not tuned in. But, the readhesion controller must be there and then the Kalman filter incorrect behaviour has to be taken into account.

In Fig. 9, there is shown a detail of measured speed. The measured speed waveform parameters are important for the correct setting of the covariance matrix R . The Kalman filter is strongly dependent on the setting of the covariance matrix R .

5.1 Simulation results and covariance matrices settings influence

The Kalman filter is applied to measured data. The Kalman filter input is only single wheelset velocity. The

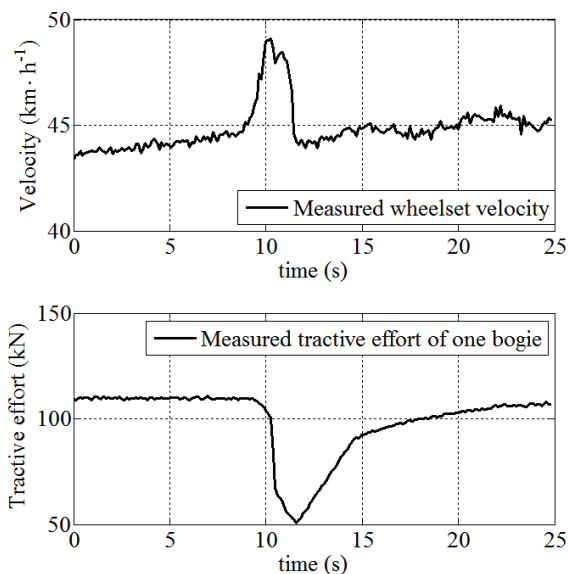


Fig. 8. Example of measured data

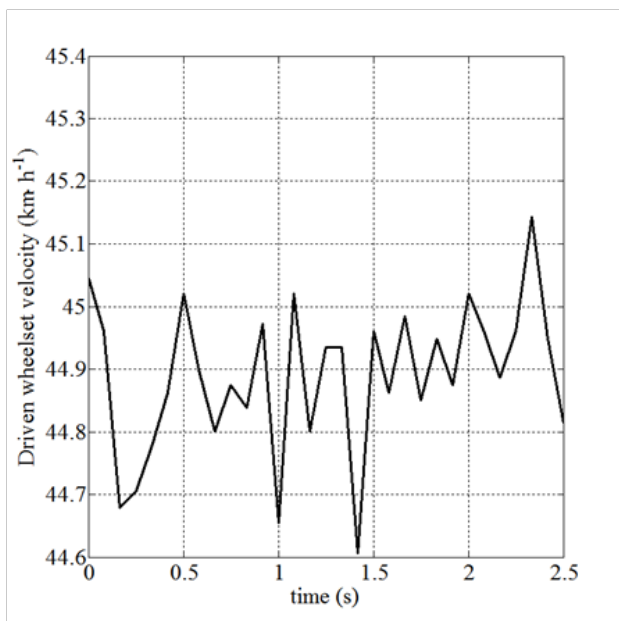


Fig. 9. Detail of measured speed

actual traction effort is for Kalman filter unknown. The Kalman filter output is shown in Fig. 10, Fig. 11 and Fig. 12 for different covariance matrices settings.

For Kalman filter correct function, it is needed to set covariance matrices of the process noise Q and covariance matrix of the measurement uncertainty R . If the matrices

are set incorrectly the Kalman filter output could be wrong. In Fig. 10, Fig. 11 and Fig. 12, the simulation results of the designed Kalman filter are shown. The filter input is the wheelset velocity and filter output is the adhesion force. In Fig. 10, Fig. 11 and Fig. 12, the measured wheelset velocities and wheelset velocities calculated by the Kalman filter are shown. The bogie tractive effort, as well as the estimated force, is also shown in the figures. The adhesion force calculated by the Kalman filter has zero value when there is no high value of the slip because the true value of the applied force is not available for the filter. If the slip velocity is low then the estimated force is zero. If the slip velocity has a high value the estimated force changes. A negative change means the decrease of the adhesion force and a positive change means the increase of the force. The big positive peaks in Fig. 10, Fig. 11 and Fig. 12 after a high value of the slip velocity are caused by the readhesion controller reaction. The controller decreases bogie tractive effort that causes an increasing of the estimated force. The estimated adhesion force has half value compared to the tractive effort that is shown in Fig. 8 because the tractive effort is for one bogie i.e. for two wheelsets and the adhesion force is for one wheelset.

The simulation results of the first covariance matrix setting is shown in Fig. 10.

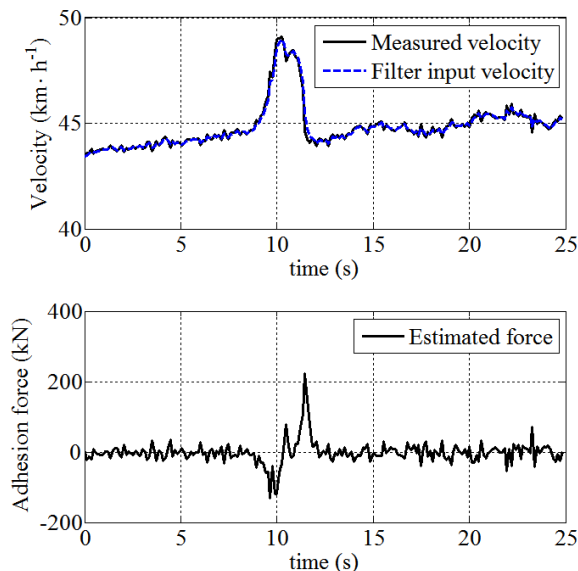


Fig. 10. Simulation results with covariance matrix set to get model agreement with measured speed

Fig. 10 shows filtered data to get match between measured wheelset velocity and filtered velocity. The covariance matrices are set to get a good match between the sig-

Table 2. Covariance matrices parameters to get model agreement with measured speed

Coefficient	value
q_1	600
q_2	50
q_3	500
q_4	200
q_5	200
q_6	200
R	40

Table 3. Covariance matrices parameters to consider speed measurement error

Coefficient	value
q_1	400
q_2	50
q_3	500
q_4	200
q_5	200
q_6	200
R	550

nals. The setting has two disadvantages. The first disadvantage is that any noise that is included in the input measured data is shown in the filter output data. The output data could be filtered by low pass filter to get more acceptable values. But, the filtration is not desirable because the data could be filtered by the Kalman filter. The second disadvantage is that the estimated adhesion force has high amplitude that is greater than the applied force during high value of the slip velocity. The covariance matrix parameters are in Table 2.

Fig. 11 shows filtered data with the covariance matrices settings to limit noise at the filter output. The input data are filtered by the Kalman filter. Therefore, the match between measured velocity and filtered velocity is not good as it is shown in Fig. 12. The set causes limitation of noise from the estimated adhesion force. The adhesion force value during high value of the slip velocity is lower. The covariance matrix parameters are in Table 3.

In Fig. 12, the simulation results for covariance matrices settings to minimize the output noise are shown. Further, it is shown that the estimated force has lower value than in Fig. 10 and Fig. 11. The high filtration causes higher output signal deformation and match between the input measured signal and filter input signal is lower. The covariance matrix parameters are in Table 4.

5.2 Covariance matrices settings

In Fig. 10, Fig. 11 and Fig. 12, the forces time courses are shown. If the change of the adhesion force is required

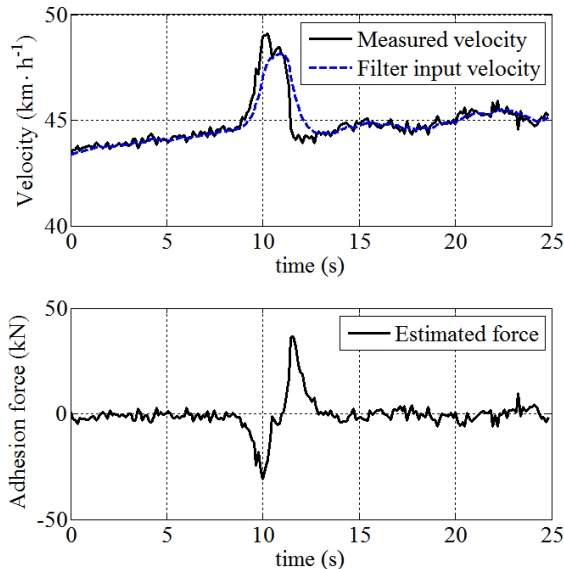


Fig. 11. Simulation results with covariance matrix settings to consider speed measurement error

Table 4. Simulation results with covariance matrix settings to minimize output noise

Coefficient	value
q_1	200
q_2	50
q_3	500
q_4	200
q_5	200
q_6	200
R	800

every time course could be used for detection of the slip velocity high value. To decide which time course has the correct value of the adhesion force, it is needed to determine the real adhesion force. The decision is based on a method that uses an observer to detect the adhesion force or adhesion coefficient [13], [14]. The force could be calculated according to the mechanical equation of the electric motor:

$$J \frac{d\omega_1}{dt} = T_M - T_L \tag{15}$$

where ω_1 is the motor angular velocity, T_M is motor torque and T_L is load torque. The estimated torque could be calculated according:

$$\hat{T}_L = \frac{a}{s+a} (T_M - J\omega_1 s) \tag{16}$$

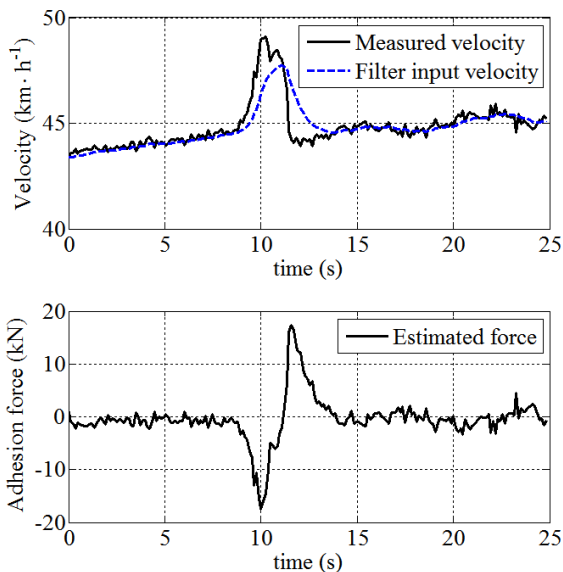


Fig. 12. Simulation results with covariance matrix settings to minimize output noise

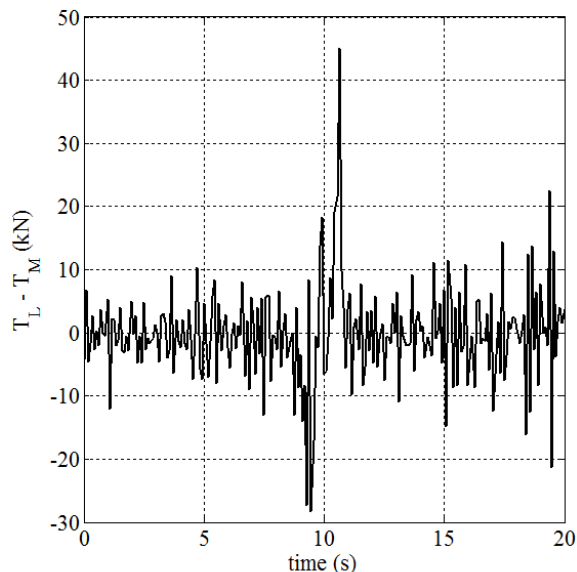


Fig. 13. Adhesion torque calculation for covariance matrix setting

where \hat{T}_L is the estimated load torque, J is the moment of inertia of all rotating part on wheelset including a gear and a motor, s is the Laplace operator and a is the observer pole.

According to the method, the difference between the motor torque and load torque is approximately 30 kN. Therefore, the simulation results according to Fig. 11 correspond with the calculation result. The covariance matrix has to be set according to data in Table 3. The calculated adhesion torque is shown in Fig. 13. The calculated torque contains noise that is caused by the measurement noise because the input data has a low filtration.

In Fig. 14, the Kalman gain K time course for the covariance matrices according to Table 3 is shown. The time courses are for first 2 seconds of simulation.

The value of measurement uncertainty covariance matrix R is connected with speed measurement properties and $R = \sigma^2$. The value of the covariance matrix could be determined from the measurement. The measurement uncertainty contains the speed sensor uncertainty. The used speed sensor is an incremental encoder. The measurement accuracy could be about $0.14 \text{ m} \cdot \text{s}^{-1}$ as shown in Fig. 9. However, it has to be considered the entire input signal uncertainty into the measurement uncertainty. The wheel acceleration during slip has the main effect in the uncertainty. The maximal wheelset acceleration can be up to $30 \text{ m} \cdot \text{s}^{-2}$. This value is calculated from eq. (15) for full motor torque and zero load torque. The real value

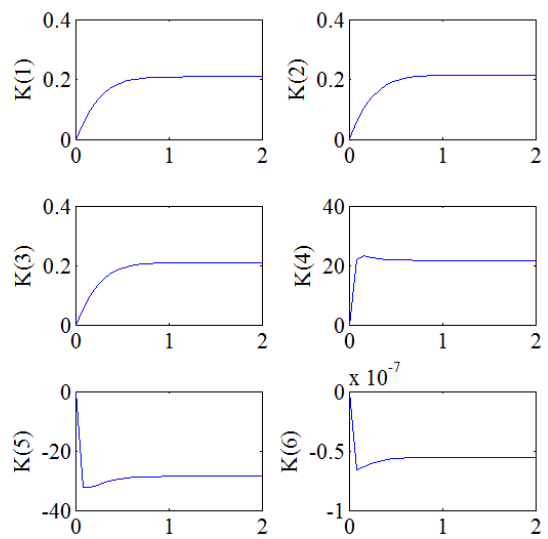


Fig. 14. Example of the Kalman gain K time course

of wheelset acceleration is from $20 \text{ m} \cdot \text{s}^{-2}$ to $25 \text{ m} \cdot \text{s}^{-2}$ for full motor torque and load torque created by adhesion force. Thus, the speed measurement variance σ should be chosen between $20 \text{ m} \cdot \text{s}^{-1}$ and $25 \text{ m} \cdot \text{s}^{-1}$.

Determination of process noise covariance matrix Q

is more difficult [12] than determination of the matrix R . Therefore, some authors determine the covariance matrix Q experimentally [15]. The matrix was determined experimentally to achieve a proper value of the adhesion force.

6 CONCLUSION

In this paper, the Kalman filter that is used for the estimation of the adhesion force that is transmitted between wheels and rails is presented. The filter uses the locomotive model that is also described in the paper. The original model has five masses but the model has to be reduced to three mass model. The reduction has to be done because the original model was unobservable. The model that is used for the time simulation is in time continues and for the Kalman filter purpose the model has to be transformed into the discrete time. Further, the Kalman filter algorithm is presented. The algorithm runs in the discrete time and the continuous time locomotive model has therefore to be transformed. The transformation is presented too. Finally, the simulation results are presented. The simulation is done using the measured wheel velocity only.

The Kalman filter output depends on the process noise covariance matrix and covariance matrix of the measurement noise matrices settings. Results for different matrix settings are presented. The measured data contain noise and the covariance matrix of the measurement noise has therefore to be set to filter the noise. However, very high degree of the filtration of the input noise could cause an undesirable distortion of the filter output signal. The time courses that represent different covariance matrices setting are presented in Fig. 10, Fig. 11 and Fig. 12. Every covariance matrix setting could be used for the high value of the slip velocity detection if the true value of the adhesion force is not required, e.g. if the method uses only derivation of the estimated adhesion force. In that case, it is appropriate to use the covariance matrix set that provides sufficient filtration to avoid using extra filter on the Kalman filter output. For the case that the true value of the adhesion force is required, the calculation of true adhesion force and the proper covariance matrix is described. The proper covariance matrix is in Table 3.

The presented slip detection method could be used for the slip value detection as a part of a locomotive slip controller.

REFERENCES

- [1] K. Ohishi, Y. Ogawa, I. Miyashita, S. Yasukawa, "Anti-slip re-adhesion control of electric motor coach based on force control using disturbance observer," *Industry Applications Conference, 2000. Conference Record of the 2000 IEEE*, vol.2, no., pp.1001,1007 vol.2, 2000.
- [2] T. Hata, H. Hirose, S. Kadowaki, K. Ohishi, N. Iida, M. Takagi, T. Sano, S. Yasukawa, "Anti-slip re-adhesion control based on speed sensor-less vector control and disturbance observer for electric multiple units, series 205-5000 of East Japan Railway Company," *Industrial Technology, 2003 IEEE International Conference on*, vol.2, no., pp.772,777 Vol.2, 10-12 Dec. 2003.
- [3] Y. Shimizu, K. Ohishi, T. Sano, S. Yasukawa, T. Koseki, "Anti-slip/skid Re-adhesion Control Based on Disturbance Observer Considering Bogie Vibration," *Power Conversion Conference - Nagoya, 2007. PCC '07*, vol., no., pp.1376,1381, 2-5 April 2007.
- [4] Y. Matsumoto, N. Eguchi, A. Kawamura, "Novel re-adhesion control for train traction system of the "Shinkansen" with the estimation of wheel-to-rail adhesive force," *Industrial Electronics Society, 2001. IECON '01. The 27th Annual Conference of the IEEE*, vol.2, no., pp.1207,1212 vol.2, 2001.
- [5] M. Yamashita, T. Soeda, "A novel slip control method considering axle-weight transfer for electric locomotive," *Vehicle Power and Propulsion Conference (VPPC), 2010 IEEE*, vol., no., pp.1,6, 1-3 Sept. 2010.
- [6] H. J. Ryoo, S. J. Kim, G. H. Rim, Y. J. Kim, M. S. Kim, "Novel anti-slip/slide control algorithm for Korean high-speed train," *Industrial Electronics Society, 2003. IECON '03. The 29th Annual Conference of the IEEE*, vol.3, no., pp.2570,2574 Vol.3, 2-6 Nov. 2003.
- [7] T. X. Mei, J. H. Yu, D. A. Wilson, "A Mechatronic Approach for Anti-slip Control in Railway Traction", *Proceedings of the 17th World Congress, The International Federation of Automatic Control*, Seoul, Korea, July 2008.
- [8] H. Yamazaki, Y. Karino, T. Kamada, M. Nagai, T. Kimura, "Effect of Wheel-Slip Prevention Control Using Nonlinear Robust Control Theory", *Quarterly Report of RTRI*, vol. 48, no. 1, pp 22,29, Feb. 2007.
- [9] K. Ohishi, Y. Ogawa, I. Miyashita, S. Yasukawa, "Adhesion control of electric motor coach based on force control using disturbance observer," *Advanced Motion Control, 2000. Proceedings. 6th International Workshop on*, vol., no., pp.323,328, 1-1 April 2000.
- [10] S. Senini, F. Flinders, W. Oghanna, "Dynamic simulation of wheel-rail interaction for locomotive traction studies," *Railroad Conference, 1993., Proceedings of the 1993 IEEE/ASME Joint*, vol., no., pp.27,34, 6-8 Apr 1993.
- [11] P. Pichlík, "Locomotive Model for Slip Control Simulation", *18th International Student Conference on Electrical Engineering*, May 2014.
- [12] M. S. Grewal, A. P. Andrews *Kalman Filtering Theory and Practice Using MATLAB*. 3rd ed. Wiley 2008.
- [13] Y. Shimizu, K. Ohishi, T. Sano, S. Yasukawa, "Anti-slip/skid re-adhesion control based on disturbance observer considering bogie vibration," *Electrical Engineering in Japan*, vol.172, no.2, pp.37-46 Sept. 2010.

- [14] S. H. Park, J. S. Kim, J. J. Choi, H. Yamazaki, "Modeling and control of adhesion force in railway rolling stocks," *Control Systems, IEEE*, vol.28, no.5, pp.44,58, October 2008.
- [15] J. Musić, M. Cević, V. Zanchy, "Real-Time Body Orientation Estimation Based on Two-Layer Stochastic Filter Architecture," *Automatika*, vol.51, no.5, pp.264,274, 2010.



Petr Pichlík received his bachelor and the master degree in electrical engineering from the Czech Technical University in Prague in 2008 and 2011 respectively. He is currently a Ph.D student and a research worker in CTU in Prague, faculty of Electrical Engineering, Department of Electric Drives and Traction. His research areas of interest are electric railway traction vehicles, locomotive slip control and digital control systems.



Jiří Zděnek Jiří Zděnek received the master degree in electrical engineering from the Czech Technical University in Prague in 1974 and Ph.D. degree in 1987. He is currently research worker in CTU in Prague, faculty of Electrical Engineering, Department of Electric Drives and Traction. His research areas of interest are electric traction vehicles, digital control systems, embedded computer hardware and real time control software.

AUTHORS' ADDRESSES

Petr Pichlík

Jiří Zděnek, Ph.D.

Department of Electric Drives and Traction,

Faculty of Electrical Engineering,

Czech Technical University in Prague,

Technická 2, 166 27 Prague, Czech Republic

email: pichlpet@fel.cvut.cz, zdenek@fel.cvut.cz

Received: 2014-12-17

Accepted: 2016-04-21